Unpolarized proton DVCS at 10.6 GeV with CLAS12 at Jefferson Lab

Journal of Physics: Conference Series **1643** (2020) 012186 doi:10.1088/1742-6596/1643/1/012186

Unpolarized proton DVCS at 10.6 GeV with CLAS12 at Jefferson Lab

Guillaume Christiaens [1,2] **for the CLAS Collaboration**

[1] University of Glasgow, Glasgow G12 8QQ, United Kingdom
[2] IRFU, CEA, Université Paris-Saclay, F-91191 Gif-sur-Yvette, France

E-mail: g.christiaens.1@research.gla.ac.uk, guillaume.christiaens@cea.fr

Abstract. Data taking with the new CLAS12 spectrometer at Jefferson Laboratory started in 2018 with a longitudinally polarized electron beam at 10.6 GeV sent on an unpolarized liquid hydrogen target. In this paper, a first glance at beam-spin asymmetry of photon electroproduction $ep \to e'p'\gamma$ from the Spring 2018 data set is presented.

1. Introduction

Defined in the 90s, the Generalized Parton Distributions (GPDs) describe the correlations between the transverse position and longitudinal momentum of a parton inside a nucleon. These GPDs are accessible via deep exclusive lepton scattering off a nucleon and offer a unique opportunity to access mass, angular momentum and pressure distributions inside the nucleon.

Among the deep exclusive processes, deeply virtual Compton scattering (DVCS) is the absorption by the nucleon target of a photon with high virtuality and the subsequent emission by this nucleon of a high-energy real photon. GPDs parameterize the DVCS amplitude through a complex integral called Compton Form Factors (CFF). This process interferes with the Bethe-Heitler process in which the high-energy real photon is emitted by the incoming or scattered lepton (see figure 1). Sending an electron beam on the proton target, the two processes interfere in the reaction $ep \to e'p'\gamma$. Through the interference of DVCS and BH, both real and imaginary part of the CFFs can be accessed providing a complete information about the DVCS amplitude.

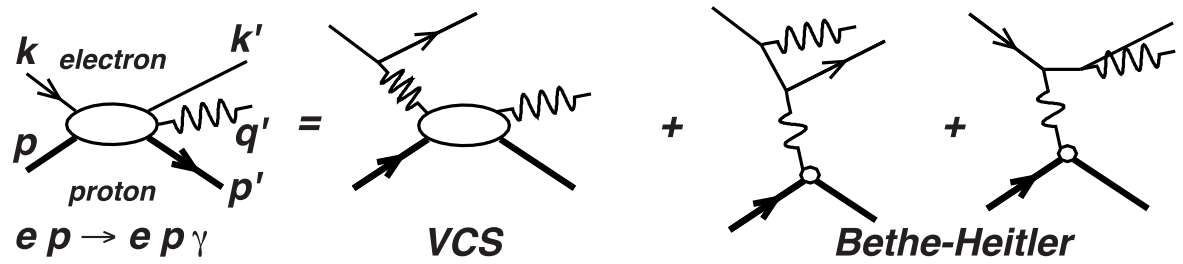

Figure 1. Photon electroproduction is made from the interferences of DVCS and Bethe-Heitler

The new CLAS12 spectrometer in the Hall B of Jefferson Laboratory has been commissioned in late 2017/early 2018. Then, for the first time, it has collected physics data with a 10.6 GeV

electron beam in Spring 2018. This large acceptance spectrometer, able to run at high luminosity, gives the best opportunity to measure accurately any observable related to the photon electroproduction over a wide kinematics phase space in order to unravel the GPDs.

From a subset of these data collected in 2018 representing about 3% of proposal statistics, a preliminary analysis of the photon electroproduction beam-spin asymmetry in the valence region is described in the following sections.

2. Theoretical and phenomenological framework

2.1. Generalized Parton Distributions

GPDs are real-functions depending on 3 variables: x the average longitudinal momentum fraction carried by the active quark, ξ the longitudinal momentum transfer to the active quark and t the squared momentum transfer to the nucleon (see figure 2). Considering only quark-helicity conserving GPDs, at leading twist, there are four GPDs: H, E, $\tilde{H}$ and $\tilde{E}$, that account for the different combinations of quark-helicity and nucleon-spin states between the initial and final state.

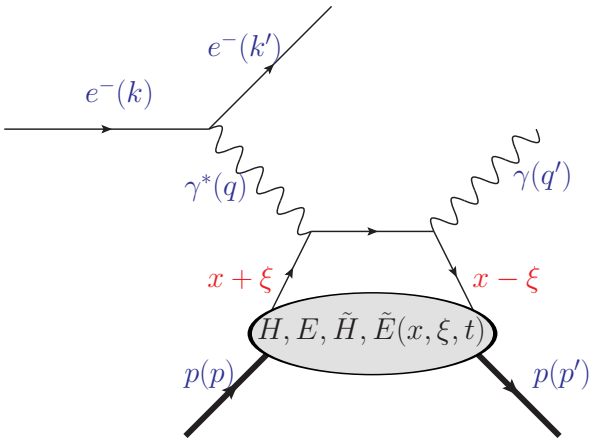

Figure 2. One of the two leading processes for the DVCS reaction. The virtuality $Q^2 = -q^2$, the Bjorken variable $x_B = \frac{Q^2}{2p.q}$, the momentum transfer to the proton $t = (p'-p)^2$ and $W^2 = (q+p)^2$ describe the DVCS reaction. The leptonic plane is defined by q and k. The hadronic plane is defined by q and q'. ϕ is the angle between the leptonic and hadronic planes.

It has been shown that, in the infinite momentum frame, there is a density interpretation related to the GPDs (not limited by relativistic effects) [1] : for instance, the impact parameter dependent parton distribution function $q(x, \boldsymbol{b}_\perp)$ is the Fourier transform of GPD $H(x, \xi = 0, t)$:

$$q(x, \boldsymbol{b}_\perp) = \int \frac{d^2\boldsymbol{\Delta}_\perp}{(2\pi)^2} H(x, 0, -\boldsymbol{\Delta}_\perp^2) e^{-i\boldsymbol{b}_\perp \cdot \boldsymbol{\Delta}_\perp} \tag{1}$$

where $\boldsymbol{b}_\perp$ is the transverse position relative to the transverse center of momentum and $\boldsymbol{\Delta}_\perp$ is the transverse momentum transfer to the proton. This interpretation allows for a 3-dimensional tomographic picture of the nucleon.

In addition, GPDs are also related to the total orbital angular momentum of quarks and gluons as described by the Ji sum rule [2]:

$$J^f = \frac{1}{2} \int_{-1}^{1} dx\, x \Big[H^f(x, \xi, \Delta^2) + E^f(x, \xi, \Delta^2) \Big]_{\Delta^2=0}, \tag{2}$$

where f stands for the flavor of the parton.

2.2. Photon electroproduction and DVCS

Photon electroproduction amplitude is the coherent sum of DVCS and BH amplitudes. It is therefore written as:

$$|A_{ep\to ep\gamma}|^2 = |A_{DVCS}|^2 + |A_{BH}|^2 + I_{DVCS/BH} \tag{3}$$

In this decomposition the BH term can be accurately computed with a parameterization of the form factors (FF). DVCS amplitude is parameterized by CFFs. As a consequence, the interference term depends on both FFs and CFFs. A Fourier expansion of each term with respect to ϕ (see Figure 2) leads to [3]:

$$|A_{DVCS}|^2 \propto c_0^{DVCS} + \sum_n \Big(c_n^{DVCS} cos(n\phi) + s_n^{DVCS} sin(n\phi) \Big) \tag{4}$$

$$|A_{BH}|^2 \propto c_0^{BH} + \lambda s_1^{BH} sin(\phi) + \sum_n \Big(c_n^{BH} cos(n\phi) \Big) \tag{5}$$

$$I_{DVCS/BH} \propto c_0^{I} + \sum_n \Big(c_n^{I} cos(n\phi) + \lambda s_n^{I} sin(n\phi) \Big) \tag{6}$$

where λ is the beam helicity. In the decomposition, the coefficients c_n^{DVCS} and s_n^{DVCS} are bilinear combinations of CFFs while c_n^I, s_n^I are linear combinations of the product between real or imaginary part of CFFs and FFs.

2.3. Beam-spin asymmetry

By keeping only leading-twist and leading-order terms, the beam-helicity dependent part of the photon electroproduction is reduced to s_1^I. Consequently, the beam-spin asymmetry simplifies to:

$$A_{LU} = \frac{\sigma(\lambda=1) - \sigma(\lambda=-1)}{\sigma(\lambda=1) + \sigma(\lambda=-1)} \tag{7}$$

$$A_{LU} = \frac{A sin(\phi)}{1 + B cos(\phi)} \tag{8}$$

where

$$A = \frac{s_1^I}{\kappa c_0^{BH} + c_0^I} \tag{9}$$

$$B = \frac{\kappa c_1^{BH} + c_1^I}{\kappa c_0^{BH} + c_0^I} \tag{10}$$

and where κ is a function of kinematical variables only.

3. Experiment

3.1. Data taking

Data in this analysis were collected in 2018 and 2019 with the CLAS12 spectrometer at Jefferson Lab. The 10.6 GeV longitudinally polarized electrons scattered off protons of a liquid hydrogen target to study photon electroproduction. The instantaneous luminosity was 6.6×10^{34} cm^{-2}s^{-1}.

3.2. CLAS12

The CLAS12 spectrometer is divided into two parts: a forward region to detect particles scattered at an angle between 5° and 35° relative to the beam direction and a central region covering angles from 35° to 125°.

The tracking system in the forward region is formed of drift chambers immersed in a toroidal magnetic field. A forward time-of-flight detector (FTOF), a High-Threshold Cherenkov counter (HTCC), an electromagnetic calorimeters (ECAL) and a pre-shower calorimeter (PCAL) provide particle identification. In the central region, the tracking system is made of the association of silicon and Micromegas detectors inside a 5T-solenoidal magnetic field and particle identification is given by a time-of-flight detector.

3.3. Particle identification

CLAS12 reconstruction package provides a basic particle identification which was used in this analysis. The electron identification relies on the matching of a negatively charged track in the drift chambers, and signals in the Cherenkov counters (at least 2 photoelectrons in the HTCC), the electromagnetic calorimeters (at least 60 MeV deposited in the PCAL and a sampling fraction (total energy deposit in ECAL and PCAL divided by the particle momentum) within the cuts shown in figure 3 and a hit in the FTOF detector. Protons are reconstructed from a positively charged track (in the forward or the central region) and a hit in one of the time-of-flight detectors: considerations on the correlations of their momentum and β-parameter provide a separation between positively charged hadrons (figure 4). Finally, photons are identified in the electromagnetic calorimeter and separation from neutrons is made from timing considerations as well (with a β cut at 0.9 in the forward detector) .

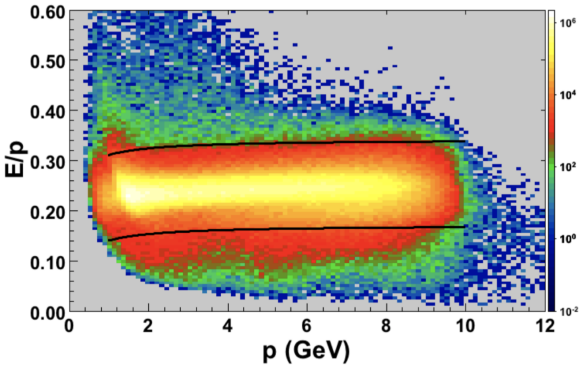

Figure 3. Sampling fraction (total energy deposition in ECAL and PCAL divided by the momentum) as a function of momentum for electrons. The black lines represent the 5-sigma cut applied for electrons identification.

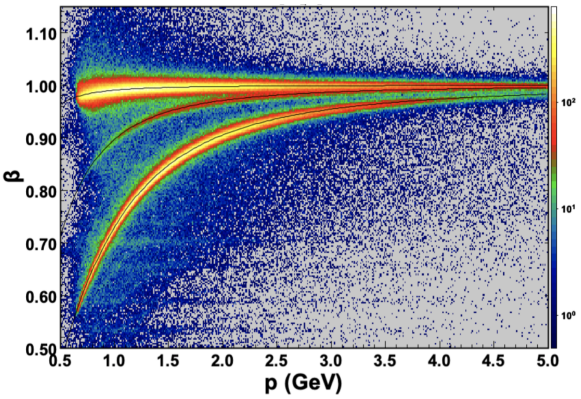

Figure 4. $\beta = v/c$ as a function of momentum for positive charges in the forward time-of-flight detector used for charged hadrons identification.

4. Analysis

4.1. Selection and exclusivity

The first step of the data analysis was the selection of events with one electron and at least one proton and one photon. The deep inelastic regime is selected with the cuts by requiring $Q^2 > 1GeV^2$ and $W^2 > 4GeV^2$. In order to ensure the exclusivity, cuts were applied on the three following variables:

- the squared missing mass $MM^2_{ep->ep\gamma X} = (k + p - k' - p' - q')^2$,

- the missing energy $ME_{ep->ep\gamma X} = (k_E + p_E - k'_E - p'_E - q_E)$,
- and the so-called photon cone angle $\theta_{\gamma X}$ (angle between the measured photon and the exclusive photon reconstructed using the proton and electron) ,

where k, k', p, p' and q' are the four-vectors of the particles as defined in figure 2. The distributions and the consequences of these cuts are shown in Fig. 5.

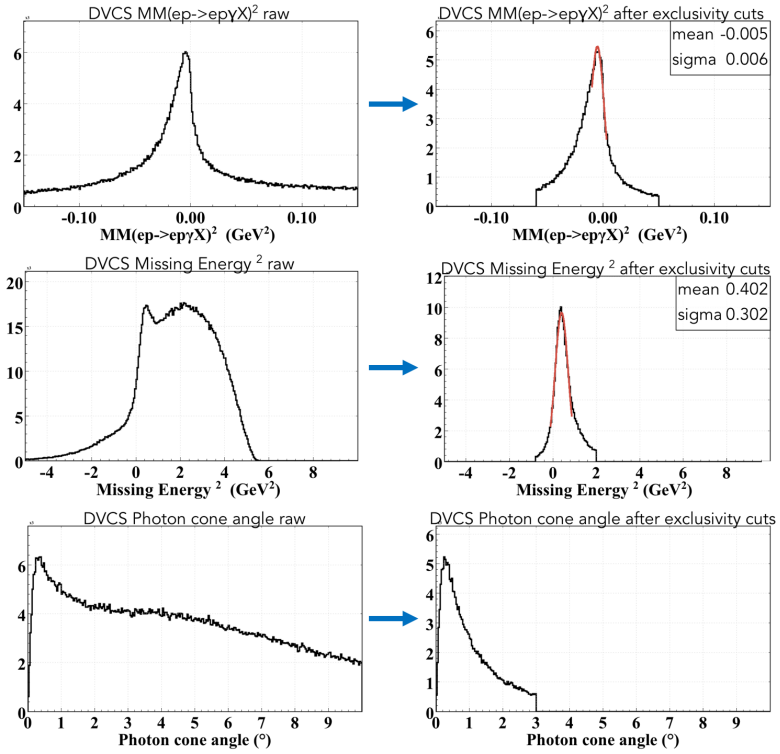

Figure 5. Exclusivity variables: squared missing mass at the top, missing energy at the middle and photon cone angle at the bottom before exclusivity cuts (left) and after the three exclusivity cuts (right)

4.2. Beam-spin asymmetry

After applying exclusivity cuts, a preliminary beam-spin asymmetry can be computed using the following relation:

$$A_{LU}(\phi) = \frac{1}{P}\frac{N^+(\phi)/Q^+ - N^-(\phi)/Q^-}{N^+(\phi)/Q^+ + N^-(\phi)/Q^-} \tag{11}$$

where P is the beam polarization, $N^+(\phi)$ and $N^-(\phi)$ are the number of events with positive or negative beam helicity in a given ϕ-bin, Q^+ and Q^- being the accumulated charge with positive or negative helicity. The beam polarization has been measured with dedicated Moller runs and has been found to be 85%. In each ϕ-bin, data are integrated over Q^2, x_B and t.

The preliminary result for the ϕ-dependence of this asymmetry is shown in figure 6 with statistical errors only. The events passing the exclusivity cuts exhibit a strong beam-spin asymmetry. A fit based on equation 8 provides the amplitude of this asymmetry $A = 0.154 \pm 0.005$ (statistical error only), with a relatively similar size compared to various model predictions in the proposal [4].

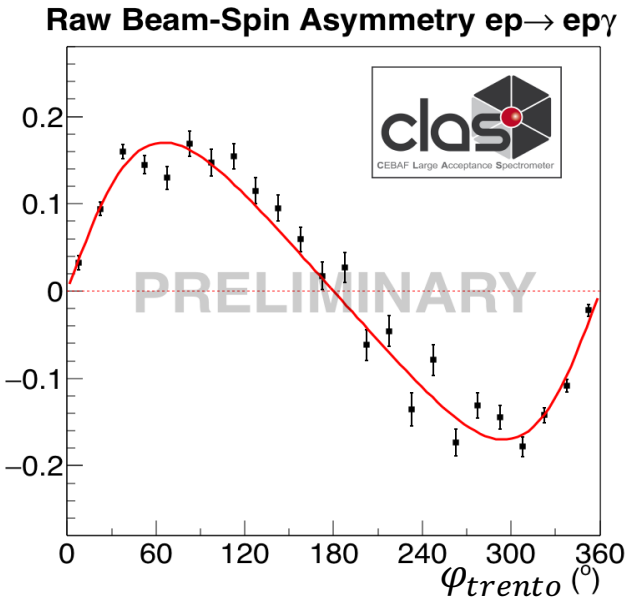

Figure 6. Preliminary ϕ dependence of the photon electroproduction beam-spin asymmetry. Error bars are statistical and the red line is a fit based on equation 8.

4.3. π^0 background

The main source of background has not been subtracted on figure 6. This background mainly comes from π^0-particles decaying into two photons: for highly-asymmetric decays with respect to the π^0-momentum in the lab frame, one of the two photons inherits almost the entire energy of the π^0-meson and mimic consequently a photon electroproduction event. Results after π^0-subtraction will be produced in a near future.

References

[1] Burkardt M 2000 *Phys. Rev.* D **62** 071503
[2] Ji X D 1997 *Phys. Rev. Lett.* **78** 610–3
[3] Belitsky A V, Mueller D and Kirchner A 2002 *Nucl. Phys.* B **629** 323–92
[4] Jefferson Lab proposal PR12-06-119: Deeply Virtual Compton Scattering with CLAS at 11 GeV. Proposal can be found here: `https://misportal.jlab.org/mis/physics/experiments/viewProposal.cfm?paperId=486`